

High-energy amplitudes of Yang-Mills theory in arbitrary perturbative orders*

Hung Cheng and C. Y. Lo

Department of Mathematics, Massachusetts Institute of Technology, Cambridge, Massachusetts 02139

(Received 14 February 1977)

In this paper, we give a summary of our work on perturbative calculations of high-energy amplitudes in Yang-Mills theory. Using the model of SU(2) with an isodoublet of Higgs bosons, we calculate the leading real part and the leading imaginary part of the vector-meson-vector-meson scattering amplitude in the 2nd through 10th orders. We also calculate two sets of diagrams to all perturbative orders: the ladder diagrams and the multi-meson-exchange diagrams. The leading terms of the amplitude of $I = 1$ (one unit of isospin exchanged) come from the ladder diagrams only and are shown to add up to a Regge-pole term corresponding to the Reggeization of the vector meson. The above results are shown to generalize easily to other non-Abelian gauge field theories. The extension to the process of fermion-fermion scattering is also straightforward, and we give a proof that these amplitudes are asymptotically proportional to the corresponding ones in vector-meson-vector-meson scattering. The 2nd- through 10th-order calculations show the following features: (i) All factors of $\ln s$ come from integration over longitudinal momenta. (ii) All divergent integrals over the transverse momenta cancel. (This has been explicitly verified up to the 8th order only.) The 2nd- through 10th-order results suggest to us a recursion formula which determines to all perturbative orders the leading terms of the scattering amplitudes. Summing up these leading terms, we found the following: (a) For the amplitude of $I = 0$ (no exchange of isospin), the sum of the leading terms exceeds the Froissart bound, representing a fixed branch point at $J_0 = 1 + [(2 \ln 2)/\pi^2]g^2$ in the plane of the angular momentum. (b) For the amplitude of $I = 2$ (two units of isospin exchanged), the sum of leading terms at $\bar{\Delta} = 0$ has a branch point at $J_2 = 2\alpha_1(0) - 1$, where α_1 is the Regge trajectory on which the vector meson lies. (c) From (a) and (b) we have $\infty > J_0 > 1 > \alpha_1(0) > J_2$. The qualitative features of high-energy scattering in Yang-Mills theories are therefore exactly the same as those in QED. In particular, the violation of the Froissart bound by summing leading terms in all these cases indicates the necessity of a calculational program to go beyond summing leading terms.

I. INTRODUCTION

The study of scattering amplitudes in QED has led to a physical picture for high-energy scattering. Some of the qualitative features are as follows:

(i) The leading terms of the $e-e$ scattering amplitude are given by the tower diagrams. They are of the order of $(e^4)(e^4 \ln s)^n$ and are imaginary, with each factor of $\ln s$ coming from the integration over the phase space of the longitudinal momentum of an $e^+ - e^-$ pair produced in the intermediate state. This means that the energy dependence of cross sections is a consequence of the creation of pionization products.

(ii) The coefficients of $(e^4)(e^4 \ln s)^n$ are in the form of convergent integrals over the transverse momenta and fractional longitudinal momenta.

(iii) The sum of these leading terms exceeds the Froissart bound, representing a fixed branch cut at $J = 1 + 11\alpha^2\pi/32$.

(iv) The photon pole does not Reggeize.

(v) The Froissart bound is restored by including all multitower diagrams.

It may appear that (iii) and (iv) are related. Specifically, the asymptotic amplitude of the diagram involving the exchange of n photons is of

the order of $s^{n\alpha-(n-1)}$ times logarithmic factors of s , where α is the singularity representing the photon in the angular momentum plane. Because of (iv), α for the photon is equal to unity, and the one-tower amplitudes are therefore always proportional to s multiplied by a factor of $\ln s$. Because of (i), the diagrams with n $e^+ - e^-$ pairs produced in the intermediate state yield an amplitude $s(\ln s)^n$, violating the Froissart bound if $n > 2$. (There is no cancellation among terms of different n since all terms at $t=0$, since they are related to the cross section of n -pair creation, are positive.)

Recently, Yang-Mills theories have gained increasing promise as a model for strong interactions. It is therefore of interest to study the behavior of high-energy amplitudes in this theory. At first sight, these theories are as complicated as they are rich. Take, for example, the model of SU(2) theory with an isospin- $\frac{1}{2}$ Higgs boson.² There are, in addition to the vector meson W , many particles in this theory: an isoscalar meson Z , a triplet of Higgs ghosts, and a triplet of Faddeev-Popov ghosts. These particles interact and there are many kinds of vertices, making perturbative calculations very lengthy. Aside from such technical complications, there is difficulty at a more qualitative level. The vector meson has

spin 1. Thus all diagrams involving the exchange of vector mesons give an amplitude of the order of s multiplied by factors of $\ln s$ in the high-energy limit. On the other hand, since the vector meson carries isospin, exchange of isospin can take place in a scattering process. Now in the high-energy limit, the amplitudes involving exchange of isospin should be much smaller than s . Thus we require spectacular cancellations among the $s(\ln s)^n$ terms for amplitudes with isospin exchange.

The resolution of this difficulty was provided by Grisaru, Schnitzer, and Tsao.³ They found evidence that the vector meson Reggeizes into a moving trajectory. Our perturbative calculations confirm their finding. Specifically, we find that all the leading terms, of the order of $g^2 s (g^2 \ln s)^n$, are real and are of $I=1$ (one unit of isospin exchanged). These leading terms cancel one another and add up to a Regge pole $s^{\alpha_1(t)}$ with $\alpha_1(t) < 1$ for $t < 0$.

What is the consequence of this Reggeization for the amplitudes of $I=0$ or $I=2$? The amplitude of the counterpart of a tower diagram is not reduced to $s^{2\alpha_1(0)-1}$ times a factor of $\ln s$, which is always smaller than s as $\alpha_1(0) < 1$, and does not violate the Froissart bound. One may hope, therefore, that the sum of the leading terms no longer violates the Froissart bound.

This hope is not realized. In essence, what happens is that, as we sum over the perturbative orders for the amplitude of $I=0$ (no exchange of isospin), the logarithmic factors are summed into a positive power of s . This power more than compensates for the Reggeization of the vector meson, and is contributed by the phase-space region of very large transverse momenta. This conclusion is in agreement with Fadin, Kuraev, and Lipatov,⁴ who used an entirely different approach. We also find that for a process of exchange of two units of isospin the logarithmic factors are summed into a negative power, giving an amplitude of the order of $s^{2\alpha_1(0)-1}$ at $\Delta=0$ (logarithmic factors of s not included). This means that extensive cancellations among the leading terms of the $I=2$ amplitude occur.

The most important conclusion that comes out of this study appears to be that summing leading terms always violates s -channel unitarity, in Yang-Mills theories as well as in QED. Indeed, the vacuum singularity in the angular momentum plane in both theories is a fixed (not moving as t varies) branch point to the right of $J=1$:

$$\begin{aligned} J &= 1 + \frac{2 \ln 2}{\pi^2} g^2 \text{ in Yang-Mills theory} \\ &= 1 + \frac{11\pi}{32} \alpha^2 \text{ in QED.} \end{aligned}$$

This indicates a need to extend the method of summing leading terms. We have found such an extension which will be discussed in a different paper.

Since the calculations are quite complicated, we shall restrict ourselves, in this paper, to a presentation and a discussion of the results only. The details of calculations will be given in the second paper of this series.

II. PERTURBATIVE CALCULATIONS

In this section, we give a summary of the results of perturbative calculations. In order to be specific, we shall deal with the SU(2) Yang-Mills theory with an isospin- $\frac{1}{2}$ Higgs boson. (The Higgs mechanism is invoked so that the vector mesons become massive—hence the complication of infrared divergence is avoided.) Extension to SU(n) is trivial, as manipulations of the isospin factors involve mainly the application of Jacobi's identity and the triangle contraction, which hold for SU(n) as well as SU(2). A brief discussion of this extension will be given in Appendix A.

In the approximation of summing leading terms, the helicities of the incident particles, measured in the c.m. system, are unchanged throughout the scattering process. We shall therefore address ourselves to the amplitude of non-helicity-flip only. For W - W scattering, we express the non-helicity-flip amplitude as

$$\begin{aligned} \mathfrak{M}_{WW} &= \left[\frac{1}{3} \delta_{\alpha\beta} \delta_{\gamma\delta} G_0 + \frac{1}{2} (\delta_{\alpha\gamma} \delta_{\beta\delta} - \delta_{\alpha\delta} \delta_{\beta\gamma}) G_1 \right. \\ &\quad \left. + \frac{1}{2} (\delta_{\alpha\gamma} \delta_{\beta\delta} + \delta_{\alpha\delta} \delta_{\beta\gamma} - \frac{2}{3} \delta_{\alpha\beta} \delta_{\gamma\delta}) G_2 \right]. \quad (1) \end{aligned}$$

In (1), α , β , γ , and δ are the isospin indices of the vector meson W as illustrated in Fig. 1. The invariant amplitude G_n is chosen so that it represents the scattering process with the exchange of n units of isospin between particle 1 and particle 1'. We shall call it the amplitude of $I=n$. The projection operator of the isospin is properly normalized. There are three independent ampli-

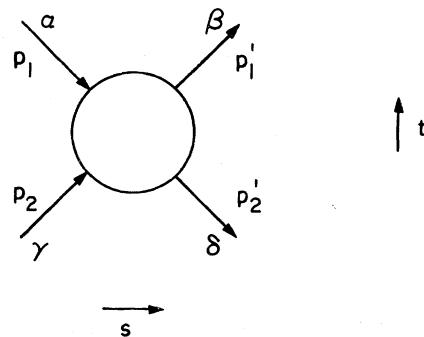


FIG. 1. Schematic diagram of the elastic scattering process.

tudes in (1) because a vector meson is of $I=1$, and particles 1 and 1' can form a state of $I=0, 1$, or 2 in the t channel.

The amplitude \mathfrak{M}_{ww} is invariant under the transformation of particle 1 \leftrightarrow particle 1', or, more explicitly

$$\alpha \leftrightarrow \beta, \quad s \rightarrow u.$$

By (1), this invariance leads to

$$G_n(s, t, u) = (-1)^n G_n(u, t, s). \quad (2)$$

In other words, under the transformation $s \rightarrow u$, G_0 and G_2 do not change, while G_1 changes sign.

It follows from (2) that in any given perturbative order the imaginary parts of the leading terms of G_0 and G_2 are of a factor $\ln s$ larger than their real parts. Indeed, under the transformation $s \rightarrow u$, we have, in the limit $s \rightarrow \infty$,

$$s \rightarrow -s, \quad \ln(se^{-i\pi}) \rightarrow \ln s. \quad (3)$$

Thus, from (2) and (3) the leading terms of G_0 and G_2 in the $(2n+2)$ th order are proportional to

$$s[\ln^n s - \ln^n(se^{-i\pi})] \sim smn \left[i \ln^{n-1} s + \frac{(n-1)\pi}{2} \ln^{n-2} s \right], \quad (4)$$

which means that the imaginary part dominates over the real part by a factor $\ln s$. Similarly, the leading term of G_1 in the $(2n+2)$ th order is proportional to

$$s[\ln^n s + \ln^n(se^{-i\pi})] \sim 2s \left(\ln^n s - \frac{ni\pi}{2} \ln^{n-1} s \right), \quad (5)$$

which says that the real part of the leading term of G_1 is larger than its imaginary part by a factor $\ln s$.

The non-helicity-flip amplitude for fermion-fermion scattering is written as

$$\mathfrak{M}_{ff} = 2^{-4} m^{-2} (F_0 - \vec{\tau}^{(1)} \cdot \vec{\tau}^{(2)} F_1), \quad (6)$$

where m is the mass of the fermion and $\vec{\tau}^{(i)}$ are the Pauli matrices (for isospin) of the fermion. The amplitude \mathfrak{M}_{ff} involves F_0 and F_1 corresponding to $I=0$ and $I=1$, respectively, because the fermion is an isodoublet. The leading terms of F_0 (F_1) in all perturbation orders are equal to those of G_0 (G_1) multiplied by a constant. These constants of proportionality are given explicitly by (19) and (20) below. A proof of this proportionality is given in Appendix A.

A. 2nd order

The 2nd-order amplitude is simple. Let us first assume that the helicities of the incoming vector mesons are either +1 or -1 (transverse polarization). Then the only contributing diagram

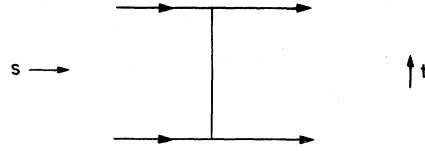


FIG. 2. The one-meson-exchange diagram for W - W scattering—the only 2nd-order diagram contributing to the leading terms. For fermion-fermion scattering, the two horizontal lines should be replaced by fermion lines.

is the one illustrated in Fig. 2. It gives

$$F_1^{(2)} \sim \frac{1}{2} G_1^{(2)} \sim \frac{2g^2 s}{\bar{\Delta}^2 + \lambda^2}, \quad (7)$$

$$F_0^{(2)} \sim G_0^{(2)} \sim G_2^{(2)} \sim 0. \quad (8)$$

In the above, λ is the mass of W and $\bar{\Delta}^2 = -t$ is the momentum transfer squared. The superscripts denote the perturbative order. Equation (7) represents the contribution of the W pole. Since the vector meson is of $I=1$, the diagram in Fig. 1 does not contribute to F_0 , G_0 , and G_2 . Note that the amplitude in (7) is proportional to s has a pole at $t = \lambda^2$, attesting to the fact that the vector meson is of $J=1$ and is a physical particle.

The equations above for the G functions hold only if both incident W mesons are of transverse polarization. If one or both of the incident W mesons are of longitudinal polarization (of helicity zero) the calculations are slightly more complicated as there is more than one contributing diagram in the Feynman gauge used throughout our calculations. The result, however, is simple:

For each of such W mesons, a factor of $\frac{1}{2}$ should be multiplied by the expressions for G . In fact, this is true for not only the leading terms of the 2nd order, but also those of arbitrary orders. With this understanding, we shall, from now on, address ourselves to W mesons of transverse polarizations only.

B. 4th order

In the 4th order, there are two diagrams contributing to the $g^4 s \ln s$ terms of the scattering amplitude. They are the box diagram and the crossed box diagram illustrated in Fig. 3. The

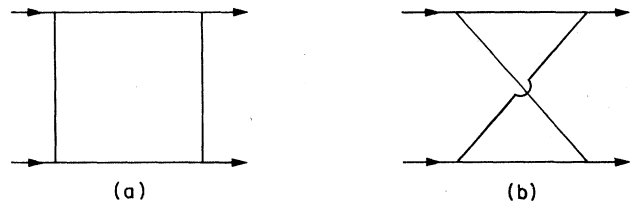


FIG. 3. The two-meson-exchange diagrams—the only 4th-order diagrams contributing to the leading terms.

calculation of the amplitude corresponding to the crossed box diagram of Fig. 3(b) is straightforward. Aside from the isospin factors, it is

$$2g^4 s \ln I(\vec{\Delta}), \quad (9)$$

where

$$I(\vec{\Delta}) = \int \frac{d^2 q_{\perp}}{(2\pi)^3} \frac{1}{(\vec{q}_{\perp}^2 + \lambda^2)[(\vec{\Delta} - \vec{q}_{\perp})^2 + \lambda^2]}. \quad (10)$$

We note that, because the crossed box diagram has no unitarity cuts in the s channel, (9) is real. The contribution of the box diagram illustrated in Fig. 3(a) is obtained from (9) by setting $s \rightarrow -s$, i.e.,

$$-2g^4 s \ln(-s)I(\vec{\Delta}), \quad (11)$$

where, according to (3), $\ln(-s)$ is interpreted as $\ln(se^{-i\pi})$. We note that the imaginary part of (11) is positive, as it should be. Note also that the real part of (11), of the order of $g^4 s \ln s$, is equal to the negative of (9), while the imaginary part of (11), of the order of $g^4 s$, is smaller than the real part by a factor of $\ln s$.

Unlike the case in QED, we do *not* add the amplitudes (9) and (11) together. This is because there are, in addition, isospin factors associated with the amplitudes. As far as the real part of the scattering amplitude is concerned, this is relatively easy to take care of. Since the real parts in (9) and (11) are equal and opposite, the sum of the real parts of the scattering amplitude is equal to the real parts of (11) times the difference of the isospin factors associated with Fig. 3(a) and Fig. 3(b). Because of Jacobi's identity, this difference is equal to the isospin factor of another diagram, which, in turn, is equal to the isospin factor associated with Fig. 2. This is schematically illustrated in Fig. 4 and Fig. 5. Thus we obtain the leading terms for the real part of the scattering amplitude to be

$$\begin{aligned} \text{Re}F_1^{(4)} &\sim \frac{1}{2}\text{Re}G_1^{(4)} \\ &\sim \frac{2g^2 s}{(\vec{\Delta}^2 + \lambda^2)} [-\ln s g^2 (\vec{\Delta}^2 + \lambda^2) I(\vec{\Delta})]. \end{aligned} \quad (12)$$

As before, the superscripts in (12) denote the perturbative orders. The imaginary parts of $F_1^{(4)}$ and $G_1^{(4)}$ are related to their real parts by (5). It is interesting to observe from (12) and (7) that the 2nd-order and the 4th-order amplitudes of $I=1$ alternate in sign. We shall see that, upon summing over all perturbative orders, the leading terms of F_1 and G_1 form a Regge-pole term. This Regge pole is located to the left of $J=1$ because of this alternation in sign.

As is seen from (9) and (11), the imaginary parts of the scattering amplitudes come from

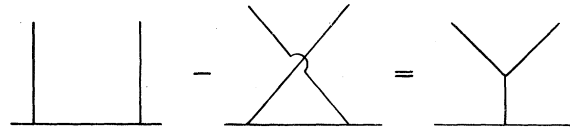


FIG. 4. The relation between the I -spin factors associated with three Feynman diagrams. The relation is a result of the Jacobi identity, and is true for any gauge theory of $SU(n)$.

diagram 3(a) only, and are of the order of s . After calculating the isospin factor of diagram 3(a), we can obtain the imaginary parts of $F_0^{(4)}$, $F_1^{(4)}$, $G_0^{(4)}$, $G_1^{(4)}$, and $G_2^{(4)}$. Although these expressions are reasonably simple, we shall not give them here. Instead, we shall list all of the 4th-through 10th-order results in Sec. II E.

Finally, we mention that there are other 4th-order diagrams, but they do not contribute to the leading terms of either the real parts or the imaginary parts of the amplitudes.

C. 6th order

For W - W scattering, there are 19 6th-order diagrams which contribute to the leading terms of $sg^2(g^2 \ln s)^2$ and $isg^4(g^2 \ln s)$. Six of them are illustrated in Fig. 6. All other diagrams can be obtained from these six diagrams either by making reflections with respect to a vertical line or a horizontal line passing through the center of the diagram, or by interchanging particle 1 with particle 1' (see Fig. 1 for notation.) We therefore need to calculate only the six diagrams in Fig. 6. The diagrams related to them by vertical or horizontal reflections give identical amplitudes. Thus we can take care of these related diagrams by multiplying the number of such diagrams by the amplitudes of the corresponding diagrams in Fig. 6. The diagrams related to the diagrams in Fig. 6 by interchanging particle 1 with particle 1' can also be taken care of easily, as will be discussed later in this subsection.

There are two technical complications in 6th-order calculations:

(i) Individual diagrams can give amplitudes as large as s^2 . Specifically, diagrams 6(a) and 6(f), and the diagrams obtained from 6(a) by particle 1 \leftrightarrow particle 1', contain s^2 terms individually.



FIG. 5. The relation (triangle contraction) between the I -spin factors associated with two Feynman diagrams. This relation can be made to hold for $SU(n)$ by appropriate definition of the coupling constant.

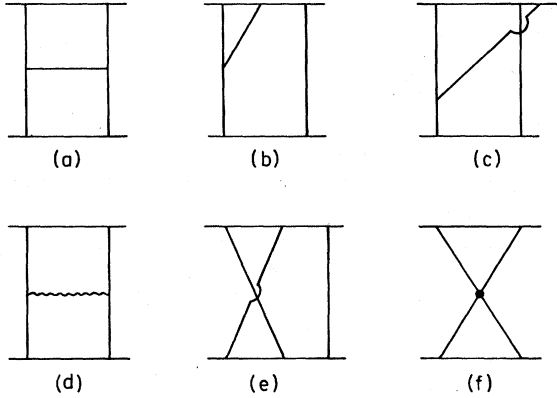


FIG 6. Examples of contributing sixth-order diagrams. The wavy line in (e) denotes the scalar meson Z which is an isoscalar.

However, these s^2 terms cancel as they are summed. We observe that diagram 6(f) is obtained from diagram 6(a) by fusing the middle rung. As a general rule, s^2 terms cancel as we add the fused diagram to the original one. It is therefore simpler if we first add the amplitudes of the fused diagrams to those of the original diagram, *before* we make asymptotic calculations. It is to be noted that there are three original diagrams which lead to the same fused diagram, corresponding to the three ways for a four-particle vertex to become

$$g^2 s \frac{[g^2 \ln(se^{-i\pi})]^2}{2!} 4I(\vec{\Delta})k, \quad (13b)$$

$$g^2 s \left\{ \frac{[g^2 \ln(se^{-i\pi})]^2}{2!} - \frac{(g^2 \ln s)^2}{2!} \right\} (-4I(\vec{\Delta})K), \quad (13c)$$

$$g^2 s \frac{[g^2 \ln(se^{-i\pi})]^2}{2!} (-\lambda^2) I^2(\vec{\Delta}), \quad (13d)$$

$$g^2 s \left\{ \frac{[g^2 \ln(se^{-i\pi})]^2}{2!} - \frac{(g^2 \ln s)^2}{2!} \right\} 4 \int \prod_{i=1}^3 \left[\frac{d^2 q_{i\perp}}{(2\pi)^2 (\vec{q}_{i\perp}^2 + \lambda^2)} \right] (2\pi)^3 \delta \left(\vec{\Delta} - \sum_{i=1}^3 \vec{q}_{i\perp} \right). \quad (13e)$$

In the above, $I(\vec{\Delta})$ is the integral given by (10) and K is a logarithmically divergent integral given by

$$K = \int \frac{d^2 q_{\perp}}{(2\pi)^3 (\vec{q}_{\perp}^2 + \lambda^2)}. \quad (14)$$

We observe that

$$\ln^2(se^{-i\pi}) - \ln^2 s = -2i\pi \ln s - \pi^2. \quad (15)$$

Thus the amplitudes given in (13c) and (13e) are actually of the order of $ig^6 s \ln s$, and are imaginary. The reason we choose to write these equations in the present form is that this makes it easy to deduce from (13a)–(13e) the asymptotic amplitudes for diagrams obtained from those in Fig. 6 by the transformation of particle 1 \rightarrow particle 1'.

“unfused.” The Feynman rule for a four-particle vertex also contains three terms and we should associate each of these terms with the corresponding original diagrams. This is discussed more fully in Appendix B.

(ii) After eliminating the s^2 terms as described above, the diagrams in Fig. 6 give leading terms of the order of $g^2 s (g^2 \ln s)^2$ and $ig^4 s (g^2 \ln s)$. The coefficients of these terms are expressed in terms of integrals over the transverse momenta. Many of these integrals are divergent. However, as we add up the contributions from all diagrams of the 6th order, all divergent integrals cancel one another and the resulting expression is convergent. This cancellation occurs in all channels ($I = 0, 1, 2$). Indeed, it occurs for other gauge field theories and is a consequence of Jacobi's identity. This is explicitly demonstrated in Appendix A.

We list the results below. The amplitude of diagram 6(a) plus the corresponding contribution of 6(f) is

$$g^2 s \frac{[g^2 \ln(se^{-i\pi})]^2}{2!} [(3\lambda^2 + 2\vec{\Delta}^2) I^2(\vec{\Delta}) - 4I(\vec{\Delta})K]. \quad (13a)$$

Diagrams 6(b), 6(c), and 6(d), and 6(e), together with the diagrams obtained from them by horizontal or vertical reflections, give the amplitudes (13b)–(13e), respectively:

Under this interchange, we see from (3) that (13c) and (13e) do not change. Together with the factor $(-1)^I$ from the transformation $\alpha \leftrightarrow \beta$, we see that, after adding the contributions of diagrams of particle 1 \rightarrow particle 1', (13c) and (13e) become proportional to

$$1 + (-1)^I, \quad (16)$$

which vanishes for $I=1$, while (13a), (13b), and (13d) become proportional to

$$s[\ln^2(se^{-i\pi}) - (-1)^I \ln^2 s]. \quad (17)$$

We shall present the calculation of the 6th-order amplitude in Appendix B and shall list the final result⁵ in subsection E. Here we shall only empha-

size the following points:

(i) The divergent integral K appears for diagrams 6(a), 6(b), and 6(c) (and the diagrams obtained from them by reflections or by particle $1 \leftrightarrow$ particle $1'$). Since the isospin factors of these three diagrams are related by Jacobi's identity, it is easy to prove that in the sum of all 6th-order diagrams, the divergent integrals K cancel. In fact, this cancellation occurs for all gauge groups.

(ii) It is of interest to observe that there are two kinds of diagrams: the ones which contribute both convergent integrals and divergent integrals to the coefficients of $g^2 s (g^2 \ln s)^2$ and $ig^4 s (g^2 \ln s)$, and the ones which contribute only divergent integrals.⁶ Diagrams 6(b) and 6(c) are of the second kind, and their contribution to the amplitude is merely to cancel out the divergent integrals from the other diagrams.

(iii) Because of (16), the diagrams of the first kind which contribute to the amplitude of $I=1$ are ladder diagrams. The leading terms for the amplitudes of $I=0$ and $I=2$ come from a larger set of diagrams and are of the order of $ig^4 s (g^2 \ln s)$.

D. 8th order

The qualitative features of the 6th-order amplitude discussed above are believed to be present for amplitudes of arbitrary orders. We have explicitly

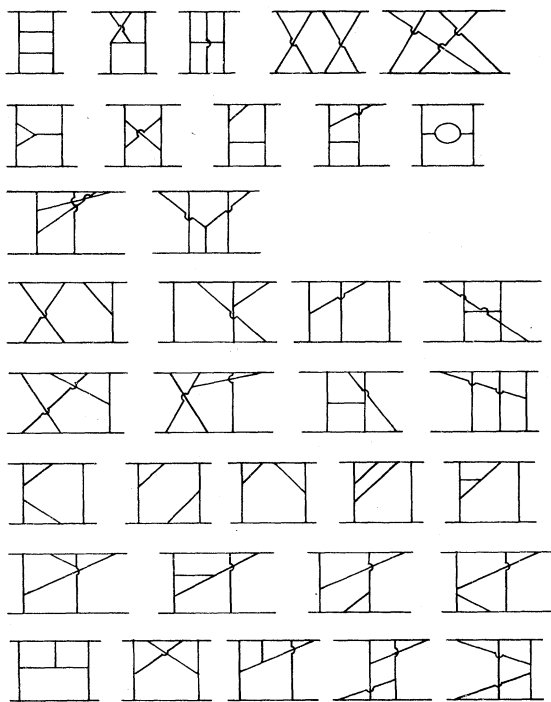


FIG. 7. The independent diagrams which contribute to the 8th-order amplitude.

verified this for the 8th-order amplitude.⁷

There are 34 independent diagrams which contribute to the leading terms of the 8th-order amplitude. They are illustrated in Fig. 7. To these diagrams we must add their horizontal and vertical mirror images, the diagrams obtained from them by making the transformation of particle $1 \leftrightarrow$ particle $1'$, and the diagrams obtained from all of the aforementioned by fusing internal lines, or replacing one or more internal lines by lines of Z mesons or Faddeev-Popov and Higgs ghosts.

Even listing the leading terms from each of the diagrams is too lengthy to do here. We shall therefore refer the reader who is interested in the details of calculations to paper II of this series. The final result is simple, and is listed in subsection E. Here we shall be content with the following remarks:

(i) Up to the 8th order, the amplitude of $I=1$ Reggeizes. We shall show in Sec. II F that this is true to all perturbative orders.

(ii) In the final result, only the following combinations of $\bar{\Delta}^2$ and λ^2 appear:

$$(\bar{\Delta}^2 + \frac{5}{4}\lambda^2), (\bar{\Delta}^2 + \lambda^2), \text{ and } (\bar{\Delta}^2 + 2\lambda^2). \quad (18)$$

Furthermore, the first and the last combinations appear exclusively in the amplitudes of $I=0$ and $I=2$, respectively.

(iii) All divergent integrals over the transverse momenta cancel.

(iv) Of the 34 diagrams illustrated in Fig. 7, only the first five are of the first kind and contribute convergent integrals to the coefficients of $g^2 s (g^2 \ln s)^3$ and $ig^4 s (g^2 \ln s)^2$. Since the separation of convergent integrals from divergent integrals is well defined,⁶ a much quicker way to obtain the final result is to calculate only these five diagrams, and extract the convergent integrals from them. Since we are unable to prove as yet that the divergent integrals cancel in all perturbative orders, we do not claim that this method is mathematically rigorous. However, we will have to resort to it for the calculation of the 10th-order amplitude, which is much too difficult to handle otherwise.

E. 10th order

As mentioned above, we shall assume that in the 10th order all divergent integrals over the transverse momenta cancel. Thus we shall calculate only those diagrams which contribute convergent integrals to the coefficients of $g^2 s (g^2 \ln s)^4$ and $ig^4 s (g^2 \ln s)^3$.

It is convenient to represent these multiple integrals over the transverse momenta by diagrams which we shall call transverse-momentum dia-

grams. These diagrams have vertices arranged in different vertical positions. There are two external lines above the highest vertex (representing particles 1 and 1') and two external lines below the lowest vertex (representing particles 2 and 2'). We shall call the lines converging on a vertex from below (above) as incoming (outgoing) lines, and the sum of momenta carried by the incoming lines the total momentum of the vertex. The total momenta of the highest or the lowest vertex are always $\vec{\Delta}$. The rules for obtaining the integral corresponding to such a diagram are as follows:

- (a) For each of the internal lines of these diagrams, there is a propagation factor $(\vec{q}_1^2 + \lambda^2)^{-1}$, where \vec{q}_1 is the transverse momentum carried by the line.
- (b) At each vertex, the transverse momentum is conserved, with the phase-space factor $d^2q_1/(2\pi)^3$.
- (c) For each horizontal bar on a vertex, there is a factor $(\vec{p}_1^2 + \lambda^2)$, where \vec{p}_1 is the total momentum flow of the vertex.

We give a simple example: The integral $I(\vec{\Delta})$, d defined by (10), is represented by the transverse-momentum diagram in Fig. 8.

We give in Table I a list of the transverse-momentum diagrams appearing in the 10th-order calculations. At the right of each of these diagrams, we list the independent Feynman diagrams which contribute to it. It is understood that all Feynman diagrams related to the ones in Table I by horizontal or vertical reflections, by making the transformation of particle 1 \leftrightarrow particle 1', by fusing one or more internal lines, or by replacing one or more internal lines by lines of Z mesons or Faddeev-Popov ghosts also be taken into account. The only exception is the last diagram in row 7 of Table I. Among the Feynman diagrams of this kind, the only contributing diagram is the one listed (the line joining the cross represents a Z meson.)

We give the summary of the 4th- through 10th-order results in Table II. Only G_0 and G_2 are listed. The 2nd- through 10th-order leading terms for the amplitude G_1 (or F_1) form the first five terms of the perturbation expansion of a Regge-pole term which will be given in the next subsection. The asymptotic forms for the functions F_I and G_I are always related by a constant multiple. Specifically,

$$F_0 \sim \frac{3}{16} G_0 \tag{19}$$

and

$$F_1 \sim \frac{1}{2} G_1 \tag{20}$$

We conclude this subsection with the following remarks:

- (i) For fermion-fermion scattering, the top and the bottom horizontal lines in the Feynman dia-

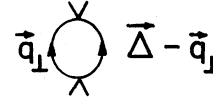


FIG. 8. The transverse-momentum diagram representing the integral $I(\vec{\Delta})$ defined by (6).

grams in Table I represent fermions.

- (ii) For W - W scattering, the top and the bottom lines in the Feynman diagrams in Table I represent vector mesons. In this case, two of the diagrams in Table I may be topologically equivalent. For example, the second and the fourth Feynman diagrams in the last row of Table I become the same after redrawing. This is illustrated in Fig. 9 (more examples are given in Fig. 10). However, in our calculations of asymptotic terms, we may treat them as distinct ones provided that we always assign the large incident momenta to pass through the top and the bottom lines.

- (iii) There are other Feynman diagrams which contribute to the fourth row of Table I, with the sum of their contribution equal to zero. There are also transverse-momentum diagrams which appear in the leading terms of individual Feynman diagrams but do not appear in the final answer. (The sum of the contribution from these Feynman dia-

TABLE I. A list of transverse-momentum diagrams appearing in the 10th-order amplitude. At the right of each of these diagrams are the independent Feynman diagrams which contribute to it. All vertices in the Feynman diagrams are three-line vertices.

Transverse momentum diagrams	Feynman diagrams

TABLE II. A summary of the 2nd- through 10th-order amplitudes. In this table, $a = 2\bar{\Delta}^2 + \frac{5}{2}\lambda^2$ and $b = \bar{\Delta}^2 + 2\lambda^2$. All vertices in the Feynman diagrams are three-line vertices.

Coef. of	$-\frac{1}{8}aG_0$	$\frac{1}{2}bG_2$
$i\pi g^4 s$	$-a\text{diagram}$	$b\text{diagram}$
$i\pi g^6 s \ell ns$	$\frac{2}{a}\text{diagram} - 2a\text{diagram}$	$b^2\text{diagram} - 4b\text{diagram}$
$i\pi g^8 s \frac{(\ell ns)^2}{2!}$	$-\frac{3}{a}\text{diagram} + 4\frac{2}{a}\text{diagram} - 2a\text{diagram} - 2a\text{diagram}$	$b^3\text{diagram} - 8b^2\text{diagram} + 8b\text{diagram} + 8b\text{diagram}$
$i\pi g^{10} s \frac{(\ell ns)^2}{3!}$	$\frac{4}{a}\text{diagram} - 6a^3\text{diagram} + 4a^2\text{diagram} + 4a\text{diagram}$ $+ 4a\text{diagram} - 4a\text{diagram} - 8a\text{diagram} - 4a\text{diagram}$ $+ 6a\text{diagram} + 2a\text{diagram}$	$b^4\text{diagram} - 12b^3\text{diagram} + 16b^2\text{diagram} + 16b^2\text{diagram}$ $+ 16b^2\text{diagram} - 8b\text{diagram} - 16b\text{diagram} - 8b\text{diagram}$ $- 24b\text{diagram} - 8b\text{diagram}$

grams vanishes.) All of them are listed in Table III.

F. The ladder diagrams and the amplitude of $I=1$

We shall give, in this subsection, the sum of leading terms of the scattering amplitudes given by the ladder diagrams. As in the 10th-order calculation, we shall extract from these diagrams only the convergent integrals for the coefficients of $g^2 s (g^2 \ell ns)^n$ and $ig^4 s (g^2 \ell ns)^{n-1}$. After we have calculated all of these leading terms, we sum them over n .

For the amplitudes of $I=1$, the result is

$$F_1 \sim \frac{1}{2} G_1 \sim \frac{g^2}{\bar{\Delta}^2 + \lambda^2} s^{\alpha_1} (1 - e^{-i\pi\alpha_1}), \quad (21)$$

where

$$\alpha_1 = 1 - g^2 (\bar{\Delta}^2 + \lambda^2) I(\bar{\Delta}), \quad (22)$$

with $I(\bar{\Delta})$ given by (10). In the physical region of s -channel scattering, $\alpha_1 < 1$. We also note from (22) that, at $t = \lambda^2$, we have $\alpha_1 = 1$. Furthermore, from (21) we see that F_1 and G_1 have poles at $t = \lambda^2$. Thus (21) represents the contribution of the Reggeized W meson. Note also that the signature of

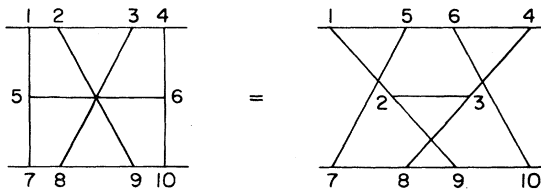


FIG. 9. An example of two equivalent diagrams for W - W scattering. All vertices are three-line vertices.

this Regge trajectory is negative. This is a consequence of crossing symmetry, as was discussed in Sec. I [see Eq. (2)].

The ladder diagrams are the only diagrams which contribute convergent integrals to the coefficients of the leading terms of F_1 and G_1 . Thus (21) gives the complete answer for the leading terms of F_1 and G_1 to all perturbative orders.

It is also possible to calculate the contribution of the ladder diagrams to the convergent part of the leading terms of G_0 , F_0 , and G_2 . We get

$$G_0^L \sim \frac{16}{3} F_0^L \sim \frac{4g^4 s^{\alpha_0}}{\bar{\Delta}^2 + \frac{5}{4}\lambda^2} (1 + e^{-i\pi\alpha_0}) \quad (23)$$

TABLE III. A list of transverse-momentum diagrams together with, at the right of each of them, the Feynman diagrams which contribute to them with the sum of contributions equal to zero. All vertices in the Feynman diagrams are three-line vertices.

Transverse momentum diagrams	Feynman diagrams

and

$$G_2^L \sim \frac{2g^4}{\bar{\Delta}^2 + 2\lambda^2} s^{\alpha_2} (1 + e^{-i\pi\alpha_2}), \tag{24}$$

where

$$\alpha_0 = 1 - g^2 (2\bar{\Delta}^2 + \frac{5}{2}\lambda^2) I(\bar{\Delta}) \tag{25}$$

and

$$\alpha_2 = 1 + g^2 (\bar{\Delta}^2 + 2\lambda^2) I(\bar{\Delta}), \tag{26}$$

with $I(\bar{\Delta})$ given by (10). Unlike (21), (23), and (24) do not include all of the leading terms of the amplitudes G_0 , F_0 , and G_2 . This is because the ladder diagrams are not the only diagrams which contribute to the leading terms of these amplitudes. Thus we use superscripts (L for ladder) for the amplitudes in (23) and (24) to distinguish them from the complete answer.

It is noted that in the physical region of s -channel scattering

$$\alpha_2 > \alpha_0.$$

This is contrary to what we expect. However, as we have mentioned, (23) and (24) are not the complete answer. We shall see in Sec. III that as the contribution of *all* other diagrams is included the situation is reversed. This is a demonstration of the kind of erroneous conclusion one can reach if one selects a particular set of diagrams as a model for high-energy scattering.

G. The multi- W -exchange amplitudes

We define the n - W -exchange diagrams to be the diagrams in which n W mesons are emitted by one of the incident particles and all of them are absorbed by the other incident particle. They are unambiguously defined for fermion-fermion scattering. Some examples of 5- W -exchange diagrams for fermion-fermion scattering can be found in the fourth row of Table I, with the top and the bottom horizontal lines representing the fermions. For W - W scattering at high energies, we calculate the same diagrams with the restriction that the large

incident momenta go through the top and the bottom lines.⁸ This set of diagrams is the counterpart of the set of multi-photon-exchange diagrams in QED, and has the characteristic of being the only set whose individual diagrams do not yield divergent transverse-momentum integrals.

It is best to begin the discussion with the 8th-order multi- W -exchange amplitudes. In this order, there are four contributing diagrams, which are illustrated in Fig. 11. Aside from the isospin factors, the amplitudes from these four diagrams are all proportional to

$$(-4) \frac{g^8 s}{4!} [\ln^4 s - \ln^4 (se^{-i\pi})] \times (\text{integral of Fig. 12}) \tag{27}$$

with the ratio of 1 : -1 : 1 : -1. Thus the sum of these four amplitudes is equal to (27) times the isospin factor

$$I_a - I_b + I_c - I_d, \tag{28}$$

where I_a is the isospin factor associated with diagram 11(a), and similarly for I_b , I_c , and I_d . The isospin factor in (28) can be easily calculated in a diagrammatic way by the use of Jacobi's identity. This is illustrated in Fig. 13.

The contributing diagrams of 5- W exchange can be obtained from the diagrams in Fig. 11 in the following way. For diagram 11(a), find the line representing the first meson emitted by the incident particle 2, which is the one joining vertex 5 and vertex 2. Assign a new vertex on the top horizontal line adjacent to vertex 2 (either at the right or at the left) and draw a line all the way to the right joining it with particle 2'. The resulting diagrams are contributing 5- W -exchange diagrams. This is illustrated in Fig. 14. Do this for all other diagrams in Fig. 11, and make reflections of all of the resulting diagrams with respect to a vertical line passing through the center of the diagram. We get all contributing 5- W -exchange diagrams. More generally, we can obtain the contributing $(n+1)$ - W -exchange diagrams from the contributing n - W -exchange diagrams in the same way.

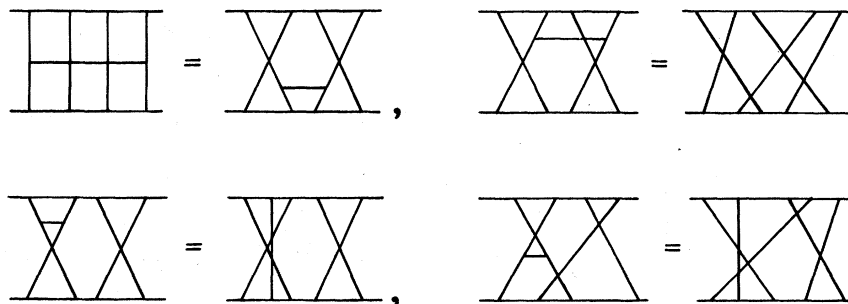


FIG. 10. More examples of equivalent diagrams for W - W scattering. All vertices are three-line vertices.

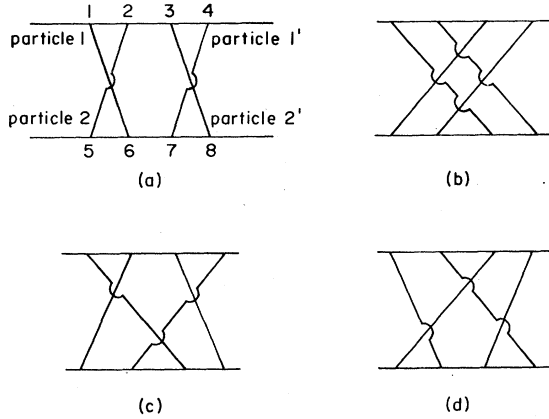


FIG. 11. The contributing 4-W-exchange diagrams.

The sum of 5-W-exchange amplitudes is proportional to a transverse-momentum integral represented by the transverse-momentum diagram in the fourth row of Table I, with the isospin factor represented by the diagram illustrated in Fig. 15. For the next higher order we simply add to the transverse-momentum diagram a line joining the vertex at the top and the vertex at the bottom and to the isospin diagram in Fig. 15 a horizontal rung.

Summing the n -W-exchange amplitudes⁹ over n for W - W scattering, we get, for $I=0$ in the t channel,

$$\frac{i}{\pi} g^4 s \int d^2 x_{\perp} e^{-i\vec{\Delta} \cdot \vec{x}_{\perp}} K_0(\lambda |\vec{x}_{\perp}|) s^{(g^2/2\pi^2)K_0(\lambda |\vec{x}_{\perp}|)} \quad (29)$$

For $n \geq 4$ the amplitude of n -W exchange is equal to the term proportional to g^{2n} in (29). However, the amplitudes of 2-W exchange and 3-W exchange are not correctly given by the g^4 and g^6 terms in (29).

For the multi-W-exchange amplitude of $I=2$, we have

$$\frac{i}{\pi} g^4 s \int d^2 x_{\perp} e^{-i\vec{\Delta} \cdot \vec{x}_{\perp}} K_0(\lambda |\vec{x}_{\perp}|) s^{-(g^2/4\pi^2)K_0(\lambda |\vec{x}_{\perp}|)} \quad (30)$$

Again, the amplitudes of 2-W exchange and 3-W exchange are the only ones not correctly incorporated in (30).

We note that the exponent of s in (29) is a function of the impact parameter \vec{x}_{\perp} . As $|\vec{x}_{\perp}|$ ranges from zero to infinity, this exponent ranges from

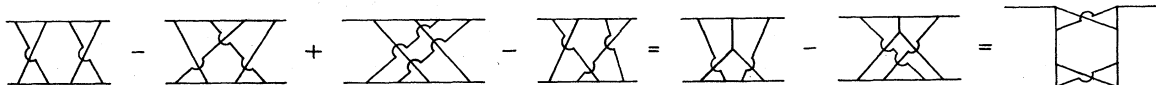


FIG. 13. Diagrammatic calculation of the isospin factor of (28). Each diagram here represents the isospin factor associated with it.



FIG. 12. The transverse-momentum diagram for 4-W exchange.

infinity to zero. Thus (29) gives a Regge singularity at $J = \infty$. Indeed, the integral in (29) is divergent if

$$s \geq e^{4\pi/g^2}.$$

As we shall see, the amplitude of $I=0$ in the t channel has a branch point at

$$J = 1 + \frac{2 \ln^2}{\pi^2} g^2$$

not at $J = \infty$, when all leading terms are taken into account. The result of summing the multi-W-exchange diagrams is again misleading.

It is trivial to obtain the multi-W amplitude for fermion-fermion scattering, or for the gauge theory of $SU(n)$. This is because the diagrammatic representation of the isospin factor, such as the one given in Fig. 15 for 5-W exchange, is derived by applying Jacobi's identity, and therefore holds for all the cases mentioned above. Thus, for any such extension, all we need to do is to calculate algebraically the isospin factor represented by these diagrams for the case under consideration.

III. LEADING TERMS TO ALL PERTURBATIVE ORDERS

In Table II, we have given the leading terms of the scattering amplitudes of $I=0$ and $I=2$ in the 4th through 10th orders. In this section, we shall use these results to deduce a recursion formula satisfied by the leading terms of consecutive orders of these amplitudes. More precisely, we shall use part of the 4th through 10th-order results to establish the recursion formula. The rest of the results serve as consistency checks.

A. Separable diagrams and factorization

We first note from Table II that there are two kinds of transverse-momentum diagrams: separable ones and nonseparable ones. A separable diagram is one which can be separated into two detached diagrams by cutting one of its vertices. All other transverse-momentum diagrams are non-

separable. We list all nonseparable transverse diagrams of 4th through 10th order in Fig. 16.

We next observe that the coefficient associated with a separable transverse-momentum diagram is factorized into a product of the coefficients associated with its nonseparable parts. For example, consider $-\frac{1}{8}aG_0$ in Table II. The coefficient associated with the two-line bubble in the second row of Table II is $(-a)$, while the coefficient associated with a series of n two-line bubbles is $(-a)^n$, where $n=2, 3$, or 4 . As another example, the coefficient associated with a three-line bubble (the 2nd diagram in the third row of Table II) is $(-2a)$, while the coefficient associated with a series of two three-line bubbles (the 3rd diagram in the fifth row of Table II) is $(-2a)^2$. In using this rule of factorization, we must remember that a separable transverse-momentum diagram can be constructed from its nonseparable parts in various ways. An example is given in Fig. 17. Thus the coefficient associated with the transverse-momentum diagram in Fig. 17 is

$$2(-a)(-2a) = 4a^2.$$

Because of factorization, the leading terms are completely determined if the coefficients associated with the nonseparable transverse-momentum diagrams are known. Furthermore, the asymptotic form of the scattering amplitude is simply expressed in terms of these coefficients. Let us set the asymptotic form of $G_I(s, \Delta^2)$ as

$$G_I(s, \Delta^2) = b_I i \pi g^4 s \sum_{n=0}^{\infty} \frac{(g^2 \ln s)^n}{n!} A_n^{(I)}(\Delta^2), \quad (31a)$$

where

$$b_0 = -\frac{4}{\Delta^2 + \frac{5}{4}\lambda^2}, \quad b_2 = \frac{2}{\Delta^2 + 2\lambda^2}; \quad (31b)$$

then $A_n^{(I)}(\Delta^2)$ is the leading term of order $2(n+2)$ listed in Table II. As we can see from Table II, $A_n^{(I)}(\Delta^2)$ contains terms represented by separable diagrams as well as terms represented by nonseparable diagrams. Let us further designate the sum of the latter as $a_n^{(I)}(\Delta^2)$.

For the purpose of relating the asymptotic form of the scattering amplitude in terms of $a_n^{(I)}(\Delta^2)$, it is somewhat earlier to deal with the Mellin trans-

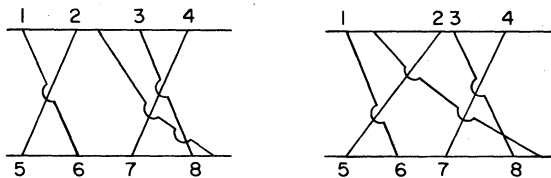


FIG. 14. The two contributing 5- W -exchange diagrams obtained from diagram 11(a).

form of (31). We set

$$\tilde{G}_I(\xi, \Delta^2) \equiv \int_1^{\infty} ds s^{-2-\xi} G_I(s, \Delta^2). \quad (32)$$

It is obvious that if

$$G_I(s, \Delta^2) \sim s^J,$$

then $\tilde{G}_I(\xi, \Delta^2)$ has a pole at

$$\xi = (J-1).$$

More generally, the asymptotic form of $G_I(s, \Delta^2)$ can be easily deduced from the location and the nature of the singularity of \tilde{G}_I in the complex ξ plane. From (31) and (32) we have

$$\tilde{G}_I(\xi, \Delta^2) \sim b_I i \pi g^2 \sum \left(\frac{g^2}{\xi}\right)^{n+1} A_n^{(I)}(\Delta^2). \quad (33)$$

By making use of factorization, we can cast (33) into

$$\tilde{G}_I(\xi, \Delta^2) = b_I i \pi g^2 \frac{h_I(\xi, \Delta^2)}{1 - h_I(\xi, \Delta^2)}, \quad (34)$$

where

$$h_I(\xi, \Delta^2) = \sum_{n=0}^{\infty} \left(\frac{g^2}{\xi}\right)^{n+1} a_n^{(I)}(\Delta^2). \quad (35)$$

B. The recursion formula

In this subsection, we shall deduce the relation between $a_n^{(I)}(\Delta^2)$ with $a_{n-1}^{(I)}(\Delta^2)$. It is obvious from Table II that the transverse-momentum diagrams associated with $a_n^{(I)}(\Delta^2)$ have one more closed loop than those associated with $a_{n-1}^{(I)}(\Delta^2)$. Thus, a recursion formula between leading terms of successive orders must involve an integration over a transverse momentum. Since $a_n^{(I)}(\Delta^2)$ does not depend on any loop momentum, let us define

$$a_n^{(I)}(\Delta^2) = \int f_n^{(I)}(\vec{\Delta}, \vec{q}_\perp) \frac{d^2 q_\perp}{(2\pi)^2}. \quad (36)$$

Equation (36) does not define $f_n^{(I)}(\vec{\Delta}, \vec{q}_\perp)$ uniquely, and we must seek guidance in the examples of our previous results. From the 4th-order results, it is most natural to define

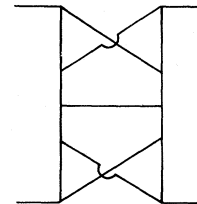


FIG. 15. The isospin factor of the sum of 5- W -exchange amplitudes is equal to the isospin factor of the diagram illustrated here.

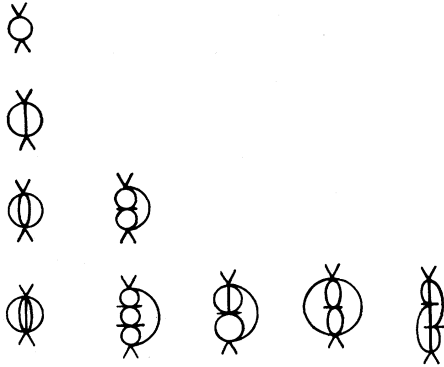


FIG. 16. A list of nonseparable transverse-momentum diagrams in the 4th-through 10th-order amplitudes.

$$f_0^{(0)}(\vec{\Delta}, \vec{q}_\perp) = -(2\vec{\Delta}^2 + \frac{5}{2}\lambda^2)(\vec{q}_\perp^2 + \lambda^2)^{-1} \times [(\vec{\Delta} - \vec{q}_\perp)^2 + \lambda^2]^{-1} \quad (37a)$$

and

$$f_0^{(2)}(\vec{\Delta}, \vec{q}_\perp) = (\vec{\Delta}^2 + 2\lambda^2)(\vec{q}_\perp^2 + \lambda^2)^{-1} \times [(\vec{\Delta} - \vec{q}_\perp)^2 + \lambda^2]^{-1}. \quad (37b)$$

We represent $-f_0^{(0)}(\vec{\Delta}, \vec{q}_\perp)/(2\Delta^2 + \frac{5}{2}\lambda^2)$ diagrammatically in Fig. 18. We note that \vec{q}_\perp and $\vec{\Delta} - \vec{q}_\perp$ are the momenta carried by the two lines in Fig. 18, respectively. Thus it is natural to represent a general term in $f_n^{(0)}(\vec{\Delta}, \vec{q}_\perp)$ by the diagram in Fig. 19. Notice that the two groups of lines in the figure carry momenta \vec{q}_\perp and $\vec{\Delta} - \vec{q}_\perp$, respectively. Since there are two equivalent ways of assigning \vec{q}_\perp and $\vec{\Delta} - \vec{q}_\perp$ to the two groups of lines, we must require $f_n^{(0)}(\vec{\Delta}, \vec{q}_\perp)$ to be unchanged under the transformation

$$\vec{q}_\perp \leftrightarrow \vec{\Delta} - \vec{q}_\perp. \quad (38)$$

As we concluded earlier, a recursion relation between $f_n^{(I)}$ and $f_{n-1}^{(I)}$ must involve an integral operation. Now since the coupling constant g^2 is dimensionless, $f_n^{(I)}$ and $f_{n-1}^{(I)}$ are of the same dimension. Thus this integral operation must preserve the dimension. Furthermore, it is obvious from Table II that a denominator factor in the kernel of this operation must be of the form of $(\vec{q}_{i\perp}^2 + \lambda^2)$, where $\vec{q}_{i\perp}$ is the momentum of a line, while a numerator factor must be of the form of $(\vec{p}_{i\perp}^2 + \lambda^2)$, where $\vec{p}_{i\perp}$ is the total momentum of a vertex. The two simplest integral operators which

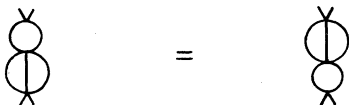


FIG. 17. Two equivalent transverse-momentum diagrams.



FIG. 18. A diagrammatic representation for $-f_0^{(0)}(\vec{\Delta}, \vec{q}_\perp)/(2\vec{\Delta}^2 + \frac{5}{2}\lambda^2)$.

satisfy these requirements are

$$(P_1 f)(q) = \int \frac{d^2 p'_\perp}{(2\pi)^3} P_1(q_\perp, q'_\perp) f(q'_\perp), \quad (39a)$$

where

$$P_1(\vec{q}_\perp, \vec{q}'_\perp) = \frac{\vec{q}'_\perp{}^2 + \lambda^2}{(\vec{q}_\perp^2 + \lambda^2)[(\vec{q}'_\perp - \vec{q}_\perp)^2 + \lambda^2]} + \frac{(\vec{\Delta} - \vec{q}'_\perp)^2 + \lambda^2}{[(\vec{\Delta} - \vec{q}_\perp)^2 + \lambda^2][(\vec{q}'_\perp - \vec{q}_\perp)^2 + \lambda^2]} \quad (39b)$$

and

$$(P_2 f)(\vec{q}_\perp) = P_2(\vec{q}_\perp) f(\vec{q}_\perp), \quad (40a)$$

where

$$P_2(\vec{q}_\perp) = (\vec{q}_\perp^2 + \lambda^2) I(\vec{q}_\perp) + [(\vec{\Delta} - \vec{q}_\perp)^2 + \lambda^2] I(\vec{\Delta} - \vec{q}_\perp), \quad (40b)$$

where $I(\vec{q}_\perp)$ is defined by (10) and diagrammatically represented by Fig. 8. Equations (39) and (40) are diagrammatically illustrated in Figs. 20 and 21. Each operation is a sum of two operations so that if f is invariant under the transformation (38), so is $P_i f$, $i=1, 2$.

The simplest operator involved in the recursion formula is a linear combination of P_1 and P_2 . It is easy to determine, by using two of the nonseparable leading terms in Table II, that the recursion formula for $I=0$ is

$$f_n^{(0)} = (2P_1 - P_2) f_{n-1}^{(0)}. \quad (41)$$

This recursion formula reproduces correctly all of the other six nonseparable leading terms in Table II.

Similarly, for $I=2$ the recursion formula is

$$f_n^{(2)} = -(P_1 + P_2) f_{n-1}^{(2)}. \quad (42)$$

We may also obtain the recursion formula for $I=1$:

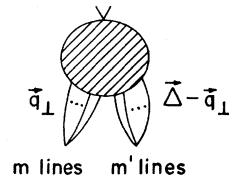


FIG. 19. A diagrammatic representation of a general term in $f_n(\vec{\Delta}, \vec{q}_\perp)$.

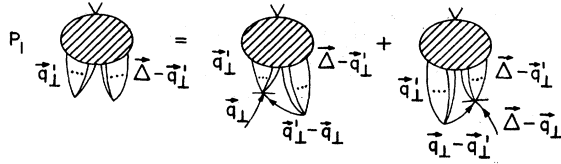


FIG. 20. Diagrammatic representation of the operator P_1 . A horizontal bar on a vertex represents a factor $(\vec{p}_\perp^2 + \lambda^2)$, where \vec{p}_\perp is the total momentum of the vertex. If there is only one outgoing line at a vertex, the horizontal bar and the outgoing line annihilate each other.

$$f_n^{(1)} = (P_1 - P_2) f_{n-1}^{(1)}. \tag{43}$$

It is easily verified that

$$(P_1 - P_2) f_0^{(1)} = 0. \tag{44}$$

Thus we have

$$f_n^{(1)} = 0, \quad n \geq 1. \tag{45}$$

Together with (34), (35), and (36), (45) means that the leading terms of G_1 add up to a Regge-pole term.

The solutions of (41) and (42), with the initial condition (37), satisfy the corresponding integral equations given by Fadın, Kuraev, and Lipatov.⁴ Since the solution of the integral equation given by these authors is not unique, our recursion relation serves the function of selecting the correct answer from these nonunique solutions.

C. The spectrum of the operators

From the recursion formulas given in the preceding subsection, it is possible to obtain the leading terms of any perturbative order. Our goal, however, is to calculate the sum of these leading

$$F_0^{(1)}(\vec{q}_\perp) \equiv \{(\vec{q}_\perp^2 + \lambda^2)[(\vec{\Delta} - \vec{q}_\perp)^2 + \lambda^2]\}^{1/2} f_0(I)(\vec{\Delta}, \vec{q}_\perp) \tag{50}$$

and

$$Q(\vec{q}_\perp, \vec{q}'_\perp) = \left\{ \frac{(\vec{q}_\perp^2 + \lambda^2)[(\vec{\Delta} - \vec{q}_\perp)^2 + \lambda^2]}{(\vec{q}'_\perp^2 + \lambda^2)[(\vec{\Delta} - \vec{q}'_\perp)^2 + \lambda^2]} \right\}^{1/2} P(\vec{q}_\perp, \vec{q}'_\perp) \\ = \frac{1}{(\vec{q}_\perp - \vec{q}'_\perp)^2 + \lambda^2} \left(\left\{ \frac{(\vec{q}'_\perp^2 + \lambda^2)[(\vec{\Delta} - \vec{q}_\perp)^2 + \lambda^2]}{(\vec{q}_\perp^2 + \lambda^2)[(\vec{\Delta} - \vec{q}'_\perp)^2 + \lambda^2]} \right\}^{1/2} + \left\{ \frac{(\vec{q}_\perp^2 + \lambda^2)[(\vec{\Delta} - \vec{q}'_\perp)^2 + \lambda^2]}{(\vec{q}'_\perp^2 + \lambda^2)[(\vec{\Delta} - \vec{q}_\perp)^2 + \lambda^2]} \right\}^{1/2} \right). \tag{51}$$

Then $Q(\vec{q}_\perp, \vec{q}'_\perp)$ is invariant under $\vec{q}_\perp \leftrightarrow \vec{q}'_\perp$, and the operator Q , defined by

$$(QF)(\vec{q}_\perp) = \int \frac{d^2q'_\perp}{(2\pi)^3} Q(\vec{q}_\perp, \vec{q}'_\perp) F(\vec{q}'_\perp), \tag{52}$$

is symmetric. Equations (48) and (49) can then be written as

$$h_0(\xi, \Delta^2) = g^2 \int \frac{d^2q_\perp}{(2\pi)^3} \frac{1}{\{(\vec{q}_\perp^2 + \lambda^2)[(\vec{\Delta} - \vec{q}_\perp)^2 + \lambda^2]\}^{1/2}} \frac{1}{\xi - g^2(2Q - P_2)} F_0^{(0)}(\vec{q}_\perp) \tag{53}$$

and

$$h_2(\xi, \Delta^2) = g^2 \int \frac{d^2q_\perp}{(2\pi)^3} \frac{1}{\{(\vec{q}_\perp^2 + \lambda^2)[(\vec{\Delta} - \vec{q}_\perp)^2 + \lambda^2]\}^{1/2}} \frac{1}{\xi + g^2(Q + P_2)} F_0^{(2)}(\vec{q}_\perp). \tag{54}$$

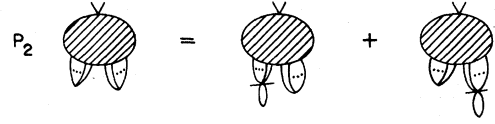


FIG. 21. Diagrammatic representation of the operator P_2 .

terms. A glance at Table II is sufficient to convince us that the way to achieve this goal is not to grind out these complicated expressions of very high orders. Let us, instead, observe that the recursion relation gives

$$f_n^{(0)} = (2P_1 - P_2)^n f_0^{(0)} \tag{46}$$

and

$$f_n^{(2)} = (-P_1 - P_2)^n f_0^{(2)}. \tag{47}$$

Thus (35) and (36) give

$$h_0(\xi, \Delta^2) = g^2 \int \frac{d^2q_\perp}{(2\pi)^3} \frac{1}{\xi - g^2(2P_1 - P_2)} \times f_0^{(0)}(\vec{\Delta}, \vec{q}_\perp) \tag{48}$$

and

$$h_2(\xi, \Delta^2) = g^2 \int \frac{d^2q_\perp}{(2\pi)^3} \frac{1}{\xi + g^2(P_1 + P_2)} \times f_0^{(2)}(\vec{\Delta}, \vec{q}_\perp). \tag{49}$$

The kernel $P_1(\vec{q}_\perp, \vec{q}'_\perp)$, defined by (39b), is not invariant under the transformation $\vec{q}_\perp \leftrightarrow \vec{q}'_\perp$. Thus P_1 is not a symmetric operator. For the purpose of the following discussion, it is convenient to symmetrize it. Let us set

We note from (50) and (37) that $F_0^{(j)}(\tilde{q}_1)$ is invariant under the transformation $\tilde{q}_1 \leftrightarrow \tilde{\Delta} - \tilde{q}_1$.

From (53), we see that for $h_0(\xi, \Delta^2)$ the location of the leading singularity in the ξ plane is equal to g^2 times the *largest* eigenvalue of the eigenfunctions of $(2Q - P_2)$ which are even under the transformation $\tilde{q}_1 \leftrightarrow \tilde{\Delta} - \tilde{q}_1$. (There is, however, an important clarification which we shall make later.) And from (54), we see that for $h_2(\xi, \Delta^2)$ the location of the leading singularity is equal to the negative of g^2 times the *smallest* eigenvalue of the eigenfunctions of $(Q + P)$ which are even under the transformation $\tilde{q}_1 \leftrightarrow \tilde{\Delta} - \tilde{q}_1$.

We shall treat only the simple case of $\tilde{\Delta} = 0$ here. In this case, it is easy to find the smallest eigenvalue of $Q + P_2$ and we shall do it first. Let us therefore try to find the minimum of

$$\int f(\tilde{q}_1)(Qf)(\tilde{q}_1) d^2q_\perp + \int f^2(\tilde{q}_1)P_2(\tilde{q}_1) d^2q_\perp \tag{55}$$

with

$$\int f^2(\tilde{q}_1) d^2q_\perp = 1,$$

where f is a trial function. At $\tilde{\Delta} = 0$,

$$Q(\tilde{q}_2, \tilde{q}'_2) = \frac{2}{(\tilde{q}_1 - \tilde{q}'_1)^2 + \lambda^2}, \tag{56}$$

which is a function of $(\tilde{q}_1 - \tilde{q}'_1)$. The eigenvalues and the eigenfunctions of the operator Q can therefore be obtained by a Fourier transform. We easily find that the spectrum of Q is $(0, \infty)$. [Indeed, the eigenvalues of Q are given by $K_0(\lambda b)/\pi$, with $0 \leq b \leq \infty$, where K_0 is the modified Bessel function.] Thus the first integral in (55) is non-negative. Next, we find from (40b) that $P_2(\tilde{q}_1)$ at $\tilde{\Delta} = 0$ has a minimum value

$$2\lambda^2 I(0), \tag{57}$$

which occurs at $\tilde{q}_1 = 0$. Thus the minimum value of (55) is (57), which is achieved by using a function $f(\tilde{q}_1)$ localized at $\tilde{q}_1 = 0$. Specifically we may consider the function

$$f(\tilde{q}_1) = \frac{1}{\epsilon} \frac{1}{\sqrt{\pi}}, \quad |\tilde{q}_1| < \epsilon \\ = 0, \quad \text{otherwise}$$

and take the limit $\epsilon \rightarrow 0$. In this limit, the first integral of (55) is zero and the second integral of (55) is equal to (57). By (22), we can express (57) in terms of $\alpha_1(0)$. Thus we find that the leading singularity of $h_2(\xi, \Delta^2)$ occurs at

$$\xi = 2\alpha_1(0) - 2, \tag{58}$$

which is the location of the singularity due to the exchange of two Regge poles α_1 .

We now turn our attention to the largest eigenvalue of $2Q - P_2$ at $\tilde{\Delta} = 0$. Let us write down explicitly the eigenequation of this operator:

$$\beta\phi(\tilde{q}_1) = 4 \int \frac{d^2q'_1}{(2\pi)^3} \frac{\phi(\tilde{q}'_1)}{(\tilde{q}_1 - \tilde{q}'_1)^2 + \lambda^2} - 2(\tilde{q}_1^2 + \lambda^2)I(\tilde{q}_1)\phi(\tilde{q}_1), \tag{59}$$

where β and $\phi(\tilde{q}_1)$ are the eigenvalue and the eigenfunction, respectively, for $2Q - P_2$. We shall show in Appendix C that the asymptotic form of $\phi(\tilde{q}_1)$ as $|\tilde{q}_1| \rightarrow \infty$ is

$$c_1(\tilde{q}_1^2)^{-\eta_1} + c_2(\tilde{q}_1^2)^{-\eta_2}, \quad 0 < \text{Re}\eta_1, \text{Re}\eta_2 < 1 \tag{60}$$

where c_1 and c_2 are constants and η_1 and η_2 satisfy the equation

$$\beta = -\frac{1}{2\pi^2} [\psi(\eta) + \psi(1 - \eta) + 2\gamma]. \tag{61}$$

In (61), $\gamma = 0.57721 \dots$ is Euler's constant and ψ is the logarithmic derivative of the Γ function:

It is straightforward to show that for

$$-\infty < \beta < \frac{2 \ln 2}{\pi^2} \tag{62}$$

the two roots of Eq. (61) are complex and are equal to

$$\frac{1}{2} \pm ip, \tag{63}$$

where p is a real number. For

$$\beta > \frac{2 \ln 2}{\pi^2}, \tag{64}$$

both roots of (61) are real and one of them is smaller than $\frac{1}{2}$. This means that if an eigenvalue of (59) is larger than $(2 \ln 2)/\pi^2$ the asymptotic form (60) is larger than $(\tilde{q}_1^2)^{-1/2}$, and the corresponding eigenfunction is not normalizable. Such eigenfunctions and eigenvalues do not enter when $(2Q - P_2)$ operates on the *square-integrable* function $f_0^{(0)}(\tilde{q}_1)$. (See Appendix C for more discussion on this point.) Thus the largest eigenvalue involved cannot be larger than $(2 \ln 2)/\pi^2$.

On the other hand, by choosing $f(\tilde{q}_1)$ to be the square-integrable function $(\tilde{q}_1^2 + \lambda^2)^{-1/2 - \epsilon}$, it is possible to show, after some algebra, that

$$\lim_{\epsilon \rightarrow 0} \frac{\langle f | (2Q - P_2) | f \rangle}{\langle f | f \rangle} = \frac{2 \ln 2}{\pi^2},$$

which means that the largest eigenvalue involved cannot be smaller than $(2 \ln 2)/\pi^2$. Therefore this eigenvalue must be equal to $(2 \ln 2)/\pi^2$. Since $\lim_{\epsilon \rightarrow 0} f = (\tilde{q}_1^2 + \lambda^2)^{-1/2}$ is not square-integrable, this eigenvalue belongs to the continuous spectrum. Thus the leading singularity of $h_0(\xi, \Delta^2)$ is located at

$$\xi = g^2(2 \ln 2)/\pi^2$$

or, in terms of J ,

$$J = 1 + g^2(2 \ln 2)/\pi^2 \quad (65)$$

and is a branch point.

The above argument, made for $\vec{\Delta} = 0$, can be extended to nonzero $\vec{\Delta}$. Since the argument above is based on the behavior of the eigenfunction as $|\vec{q}_\perp| \rightarrow \infty$, and since the asymptotic behaviors of the kernel $Q(\vec{q}_\perp, \vec{q}'_\perp)$ or the function $P_2(\vec{q}_\perp)$ for large values of momenta are independent of $\vec{\Delta}$, Eq. (65) is valid for all finite $\vec{\Delta}$.

By (34), a branch point of $h_I(\xi, \Delta^2)$ is also a branch point of $\tilde{G}_I(\xi, \Delta^2)$. The function $\tilde{G}_I(\xi, \Delta^2)$ has, in addition, poles at

$$h_I(\xi, \Delta^2) = 1.$$

We are unable to determine the location of these poles.

D. Summary

In summary, we have found, by summing the leading terms in the Yang-Mills theory of SU(2) with an isodoublet of Higgs bosons, the following singularities in the angular momentum plane:

(i) A fixed branch point at $J_0 = 1 + g^2(2 \ln^2)/\pi^2$ for the amplitude of no isospin exchange.

(ii) A moving Regge pole $J_1 = \alpha_1(\vec{\Delta})$ given by (22) for the amplitude with the exchange of one unit of isospin.

(iii) A Regge branch point located at $J_2 = 2\alpha_1(0) - 1$ at $\vec{\Delta} = 0$ for the amplitude with the exchange of two units of isospin.

It is interesting to observe that

$$\infty > J_0 > J_1 > J_2. \quad (66)$$

This is consistent with the experimental fact that in the high-energy limit the amplitude with the exchange of quantum numbers is much smaller than the amplitude with no exchange of quantum numbers. It is impressive that (66) is an output, instead of an input, of the theory. In fact, the way (66) comes out is quite spectacular: It requires extensive cancellations among terms of all perturbation orders. Indeed, (66) is not true if we restrict ourselves to a particular set of Feynman diagrams such as the ladder diagrams or the multi- W -exchange diagrams. There are, in addition, many physical features which are realized in the model of Yang-Mills theory: the relationship between the energy dependence of the cross sections and the creation of pionization products, the approximate conservation of helicity, and the relatively small values of the real parts of the scattering amplitudes. All of these indicate that the Yang-Mills theories are promising models for the high-energy scattering of hadrons.

There is only one undesirable feature in our result: that the amplitude with no exchange of iso-

spin violates the Froissart bound. This is by no means a weakness of Yang-Mills theories. Rather, it once again shows us that, just as in QED, the method of summing leading terms is not adequate to deal with the vacuum singularity. In a separate paper, we shall discuss a new method to deal with this situation.

APPENDIX A

The amplitude corresponding to a Feynman diagram in the gauge theory of SU(2) is equal to a space-time integral multiplied by an isospin factor. In the high-energy limit, the space-time integral is best evaluated by the method of longitudinal-momentum integration. In this appendix, we discuss a simple method—the diagrammatic method—to deal with the isospin factor.

Let us first define the isospin factor associated with a Feynman diagram. It is the factor obtained by using the rules given in the second column of Appendix B. In this appendix, we shall diagrammatically represent it by the Feynman diagram it is associated with. One of the beauties of the Yang-Mills theory as a model for high-energy scattering is that we do *not* need to calculate algebraically the isospin factor for each Feynman diagram. For the purpose of calculating the sum of amplitudes of a certain order, it is much easier to sum up the amplitudes in a diagrammatic way. Furthermore, many regularities of the amplitudes become evident only if we use the diagrammatic method. An example is the proportionality between F_I and G_I given explicitly in (19) and (20). This proportionality does not, in general, hold for the amplitude of a single diagram, but is true for the sum of all diagrams.

We shall demonstrate these points by carrying out explicitly all the steps involved in dealing with the isospin factor of the 6th order. Referring to (13), we shall define

$$(1, \pm 1) \equiv g^2 s \left\{ \frac{[g^2 \ln(s e^{-i\pi})]^2}{2!} \pm \frac{(g^2 \ln s)^2}{2!} \right\}, \quad (A1)$$

$$A \equiv (3\lambda^2 + 2\Delta^2)I^2(\vec{\Delta}) - 4I(\vec{\Delta})K, \quad (A2)$$

$$B \equiv 4I(\vec{\Delta})K, \quad (A3)$$

$$D \equiv -\lambda^2 I^2(\vec{\Delta}), \quad (A4)$$

and

$$E \equiv 4 \int \prod_{i=1}^3 \left[\frac{d^2 q_{i\perp}}{(2\pi)^3 (\vec{q}_{i\perp}^2 + \lambda^2)} \right] (2\pi)^3 \delta(\vec{\Delta} - \sum_i \vec{q}_{i\perp}). \quad (A5)$$

Equations (13a)–(13e) have included the contributions of Feynman diagrams illustrated in Fig. 6, and their horizontal and vertical mirror images. (To obtain the scattering amplitude, we must mul-

$$\begin{aligned}
\frac{1}{2} A (\text{H} - \text{X}) + \frac{1}{2} B (\text{H} - \text{X}) + \frac{1}{2} D (\text{H} - \text{X}) &= \frac{1}{2} A (\text{H} - \text{X}) + \frac{1}{2} (B+D) (\text{H} - \text{X}) \\
&= \frac{1}{2} A \text{H} + \frac{1}{2} (B+D) \text{X} \\
&= \frac{1}{2} (A+B+D) \text{I}
\end{aligned}$$

FIG. 22. Diagrammatic calculation of the coefficient of $(1, 1)$. The first step involves the use of the triangle contraction in Fig. 5. The second step involves the use of Jacobi's identity, and the third step involves the use of the triangle contraction. Manipulations involving the Z meson must be modified, if the group is $SU(n)$, if the Higgs bosons are not isodoublets.

tively these expressions by their respective isospin factors.) We must also take care of the diagrams obtained from the ones mentioned above by the transformation of particle 1 \leftrightarrow particle 1'. [The space-time integrals for these latter diagrams can be obtained from (13a)–(13e) with the aid of (3).] We shall add up all these terms diagrammatically.

We shall make use of the two identities illustrated in Figs. 4 and 5. Here we emphasize one point. Both identities remain valid if the horizontal line is a fermion line or if the gauge group of the field is $SU(n)$.

The coefficient of $[1, 1]$ is calculated in Fig. 22, and the coefficient of $[1, -1]$ is calculated in Fig. 23. All the steps involved remain true if the top and (or) the bottom horizontal lines represent fermions. In order to obtain the 6th order terms of F_i and G_i , we need to calculate only the isospin factors appearing in the final answer. It is obvious, even without such a calculation, that the divergent integrals cancel out in the final answer. This is true for W - W scattering and fermion-fermion scattering. It is also true for any Yang-Mills theory of $SU(n)$.¹⁰

We are now ready to prove the constant proportionality between F_i and G_i , $i=0, 1$. First of all, in the high-energy limit, the space-time integral associated with the Feynman diagram always changes by a factor of $(2m)^{-1}$ as one of the incident W mesons is replaced by a fermion. This is because the numerator factors associated with the fermion line carrying a large p_+ are approximately

$$\gamma_+(\not{p}+m)\gamma_+(\not{p}+m)\cdots\gamma_+\sim(2p_+)^{n-1}\left(\frac{p_+}{m}\right), \quad (\text{A6})$$

where n is the number of fermion-fermion- W vertices, and the numerator factors associated with the W line carrying a large p_+ are approximately $(2p_+)^n$. Next we turn to the isospin factor. In the case of $I=1$, the isospin factor of the sum of amplitudes is always proportional to the one in the final answer of Fig. 22. This leads to the proportional-

ity between F_1 and G_1 given by (20). For the case of $I=0$, the isospin factors in the final answer involve only the ones represented by diagrams with exactly two vertices on the top (or bottom) horizontal line, which, according to the second column in the table of Appendix B, give the isospin factor

$$\frac{\tau_a}{2} \frac{\tau_b}{2} \text{ for the fermion,} \quad (\text{A7})$$

and

$$(i\epsilon_a)(i\epsilon_b) \text{ for the } W \text{ meson.} \quad (\text{A8})$$

In the above, a and b are the isospin indices of the W meson emitted at the vertices and the matrix element of ϵ_a is

$$(\epsilon_a)_{ij} = \epsilon_{aij}.$$

To obtain F_0 and G_0 , we calculate the trace of (A7) and (A8) with proper normalizations in consistency with (1) and (6). In this way, we obtain (19).

APPENDIX B

The Feynman rules for the Yang-Mills theory of $SU(2)$ with an isodoublet of Higgs bosons have been given explicitly by 't Hooft and Veltman.² We shall list those rules in the Feynman gauge where there are no $k_\mu k_\nu$ terms in the propagator for the Yang-Mills field. We have broken up all of the four-line vertices into sums of terms such that each of them has the same isospin factor as a second-order diagram with two three-line vertices. The isospin factor is normalized such that the relation illustrated in Fig. 5 is satisfied. We list the Feynman rules in Table IV below.

APPENDIX C

In this appendix, we study the eigenvalue Eq. (59). We begin by determining the asymptotic form of the eigenfunction of (59). Let us take the limit $\vec{q}_1^2 \rightarrow \infty$ in (59) and replace $\psi(\vec{q}_1)$ by $(\vec{q}_1^2)^{-\eta}$. Then the first term in the right side of (59) becomes

TABLE IV. The first five rows of the first column represent, respectively, the fermion propagator, the vector-meson propagator, the FP ghost propagator, the Z propagator, and the four-propagator. For every closed FP ghost loop, we have an extra factor -1 . It is to be noted that there is freedom in choosing the isospin factor and the space-time factor for a vertex, as long as their product coincides with that defined in Ref. 2. For the purpose of comparing W - W scattering with f - f scattering, it is convenient to change the signs of both factors of the f - f - W vertex, if the vector meson lies at the left of the arrow on the fermion line.

Diagram	Isospin factor	Time-space factor
	/	$\frac{-(\not{k} + M)}{k^2 - M^2 + i\epsilon}$
	δ_{ab}	$\frac{g_{\mu\nu}}{k^2 - \lambda^2 + i\epsilon}$
	δ_{ab}	$\frac{-1}{k^2 - \lambda^2 + i\epsilon}$
	/	$\frac{-1}{k^2 - \mu^2 + i\epsilon} \quad \mu^2 = 4\sigma\lambda^2$
	δ_{ab}	$\frac{-1}{k^2 - \lambda^2 + i\epsilon}$
	$-\frac{1}{2} \tau_a$	$-g\gamma_\mu$
	$i\epsilon_{abc}$	$g [g_{\gamma\alpha}(q-k)_\beta + g_{\alpha\beta}(k-p)_\gamma + g_{\beta\gamma}(p-q)_\alpha]$
	$i\epsilon_{abc}$	$-g\rho_\alpha$
	$i\epsilon_{abc}$	$-g\frac{1}{2}(p-q)_\alpha$
	δ_{ab}	$g\left(-\frac{i}{2}\right)(p-q)_\alpha$
	$i\epsilon_{abc}$	$g\left(-\frac{i}{2}\right)\lambda$
	δ_{ab}	$g_{\alpha\beta}\lambda$

Diagram	Isospin factor	Time-space factor
	δ_{ab}	$g(-2\sigma\lambda)$
	/	$g(-6\sigma\lambda)$
	δ_{ab}	$g\left(-\frac{\lambda}{2}\right)$
	$(i\epsilon_{aac})(i\epsilon_{edb})$	$-g^2(g_{\alpha\beta}g_{\gamma\delta} - g_{\alpha\delta}g_{\beta\gamma})$
	$\delta_{ab}\delta_{cd}$	$g^2\frac{1}{2}g_{\alpha\beta}$
	δ_{ab}	$g^2\frac{1}{2}g_{\alpha\beta}$
	$\delta_{ac}\delta_{bd}$	$g^2(-\sigma)$
	δ_{ab}	$g^2(-\sigma)$
	/	$g^2(-\sigma)$

$$\int \frac{d^2\vec{q}'_1}{(\vec{q}'_1{}^2)^\eta [(\vec{q}'_1 - \vec{q}'_1')^2 + \lambda^2]} = \int_0^1 \frac{\pi dx x^{\eta-1} (1-x)^{-\eta}}{(x\vec{q}'_1{}^2 + \lambda^2)^\eta}, \quad (C1)$$

where x is a Feynman parameter introduced to facilitate the integration over \vec{q}'_1 . The asymptotic form of the right side of (C1) as $\vec{q}'_1{}^2 \rightarrow \infty$ is best obtained by making a Mellin transform:

$$\begin{aligned} \int_0^\infty d(\vec{q}'_1{}^2) (\vec{q}'_1{}^2)^{-\xi} \int_0^1 \frac{\pi dx x^{\eta-1} (1-x)^{-\eta}}{(x\vec{q}'_1{}^2 + \lambda^2)^\eta} &= \frac{\Gamma(1-\xi)\Gamma(\xi+\eta-1)}{\Gamma(\eta)} \int_0^1 \frac{\pi dx x^{\eta-\xi-2} (1-x)^{-\eta}}{(\lambda^2)^{\xi+\eta-1}} \\ &= \pi \frac{\Gamma(1-\xi)}{\Gamma(\xi)} \frac{\Gamma(1-\eta)}{\Gamma(\eta)} \frac{\Gamma^2(\xi+\eta)}{(\xi+\eta-1)^2 (\lambda^2)^{\xi+\eta-1}}. \end{aligned} \quad (C2)$$

In the neighborhood of $\xi = 1 - \eta$, the right side of (C2) is approximately

$$\frac{\pi}{(\xi+\eta-1)^2} - \frac{\pi}{\xi+\eta-1} [\psi(\eta) + \psi(1-\eta) + 2\gamma + \ln\lambda^2]. \quad (C3)$$

The location and nature of the singularity of the Mellin transform of a function are related to the asymptotic form of the function as $\vec{q}'_1{}^2 \rightarrow \infty$. Specifically, (C3) means that the right side of (C1) is asymptotically

$$\pi \ln \left(\frac{\tilde{q}_1^2}{\lambda^2} \right) (\tilde{q}_1^2)^{-\eta} - \pi [\psi(\eta) + \psi(1 - \eta) + 2\gamma] (\tilde{q}_1^2)^{-\eta}. \quad (C4)$$

The asymptotic form of $I(\tilde{q}_1)$ is also easily obtained from (10) and Feynman parametrization:

$$I(\tilde{q}_1) = \frac{1}{8\pi^2} \int_0^1 \frac{dx}{x(1-x)\tilde{q}_1^2 + \lambda^2} \sim \frac{1}{4\pi^2} \frac{\ln(\tilde{q}_1^2/\lambda^2)}{\tilde{q}_1^2}. \quad (C5)$$

From (C4), (C5), and (59), we conclude that η must be a root of (61).

We are unable to solve (59) in closed form. In order to gain some understanding of this equation, we shall solve it in the limit $\beta \gg 1$. Let us first carry out the angular integration in (59) and get

$$\beta\phi(\rho) = \frac{1}{2\pi^2} \int_0^\infty \frac{d\rho' \phi(\rho')}{[(\rho + \rho' + \lambda^2)^2 - 4\rho\rho']^{1/2}} - 2(\rho + \lambda^2)I(\rho)\psi(\rho), \quad (C6)$$

where

$$\rho \equiv \tilde{q}_1^2, \quad \rho' \equiv \tilde{q}_1'^2.$$

In the limit $\beta \rightarrow \infty$, the second term in the right side of (C6) is small compared to the left side of (C6), unless $\rho \gg 1$. In the limit $\rho \gg 1$, the asymptotic form (C5) holds for I . Thus we may approximate (C6) as

$$\beta\phi(\rho) \sim \frac{1}{2\pi^2} \int_0^\infty \frac{d\rho' \phi(\rho')}{[(\rho + \rho' + \lambda^2)^2 - 4\rho\rho']^{1/2}} - \frac{1}{2\pi^2} \ln \left(\frac{\rho + \lambda^2}{\lambda^2} \right) \phi(\rho), \quad (C7)$$

$$\frac{1}{\{[e^{\gamma(t-t')} - 1]^2 + 2e^{-\gamma t'}[1 + e^{\gamma(t-t')}]\}^{1/2}} \sim \frac{1}{[\gamma^2(t-t')^2 + 4e^{-\gamma t}]^{1/2}}, \quad \gamma|t-t'| \ll 1. \quad (C13)$$

We may further approximate the right side of (C13) as

$$\frac{1}{\gamma|t-t'|}, \quad (C14)$$

provided that

$$\gamma|t-t'| \gg e^{-\gamma t/2}. \quad (C15)$$

Thus the contribution of the neighborhood of $t' = t$ to the integral in (C11) is

$$\phi(t) \int_{|t-t'|=e^{-\gamma t/2}}^1 \frac{dt'}{\gamma|t-t'|} = t\phi(t). \quad (C16)$$

Substituting (C12) and (C16) into (C11), we get

$$\phi(t) \sim \int_0^t dt' e^{-\gamma(t-t')} \phi(t') + \int_t^\infty dt' \phi(t'). \quad (C17)$$

The solution of (C17) is

where the argument of the logarithm is chosen to be $(\rho + \lambda^2)/\lambda^2$ instead of ρ/λ^2 so that the logarithmic function would not blow up at $\rho = 0$. Set

$$\frac{1}{2\pi^2} \ln \frac{\rho + \lambda^2}{\lambda^2} = \beta t, \quad (C8)$$

or

$$\rho = \lambda^2(e^{\gamma t} - 1), \quad (C9)$$

where

$$\gamma = 2\pi^2\beta; \quad (C10)$$

then (C7) becomes

$$(1+t)\phi(t) \sim \int_0^\infty \frac{e^{\gamma t'} dt' \phi(t')}{[(e^{\gamma t} - e^{\gamma t'})^2 + 2(e^{\gamma t} + e^{\gamma t'}) - 1]^{1/2}}. \quad (C11)$$

We shall next make an approximation for the kernel of (C11). In the limit $\gamma \gg 1$, the kernel is approximately equal to

$$e^{-\gamma(t-t')} \text{ for } t' < t, \\ 1 \text{ for } t' > t. \quad (C12)$$

Equation (C12) does not hold in the neighborhood of $t' = t$. More precisely, (C12) holds only if $\gamma|t-t'| \gg 1$. Indeed, at $t' = t$, the kernel is equal to $\frac{1}{2}e^{\gamma t/2}$, which is an exponentially large number. Thus we must also investigate the contribution of the neighborhood of $t' = t$. In this neighborhood the kernel is approximately equal to

$$\phi(t) = \frac{e^{-\eta_1 \gamma t}}{\eta_1} - \frac{e^{-\eta_2 \gamma t}}{\eta_2}, \quad (C18)$$

where

$$\eta_1 = \frac{1}{2} - \left(\frac{1}{4} - 1/2\pi^2\beta\right)^{1/2}, \quad (C19)$$

$$\eta_2 = \frac{1}{2} + \left(\frac{1}{4} - 1/2\pi^2\beta\right)^{1/2}. \quad (C20)$$

By (C18) and (C9), the eigenfunction given by (C18) is equal to a constant times

$$\frac{(\tilde{q}_1^2 + \lambda^2)^{-\eta_1}}{\eta_1} - \frac{(\tilde{q}_1^2 + \lambda^2)^{-\eta_2}}{\eta_2}. \quad (C21)$$

These two values η_1 and η_2 are precisely the two roots of (61) in the limit $\beta \gg 1$. Comparing (60) and (C20) we find that

$$C_1 \sim \frac{1}{\eta_1}, \quad C_2 \sim \frac{1}{\eta_2}. \quad (C22)$$

$$\begin{aligned}
 & \frac{1}{2} A (\text{H} + \text{X}) + \frac{1}{2} B (\text{H} + \text{X} + 2\text{H}) + \frac{1}{2} D (\text{H} + \text{X}) + E (\text{H} + \text{X}) \\
 &= \frac{1}{2} A (\text{H} + \text{X}) + \frac{1}{2} B (\text{H} + \text{X} - \text{H} - \text{X}) + \frac{1}{2} D (\text{H} + \text{X}) + E (\text{H} - \text{X}) \\
 &= \frac{1}{2} (A+B) (\text{H} + \text{X}) + \frac{1}{2} D (\text{H} + \text{X}) + E \text{H} \\
 &= \frac{1}{2} (A+B) (\text{H} + \text{X}) + \frac{1}{2} D (\text{H} + \text{X}) \\
 &+ \frac{E}{2} (\text{H} + \text{X}) + \frac{E}{2} (\text{H} + \text{X} - \text{H} - \text{X}) \\
 &= \frac{1}{2} (A+B-E) (\text{H} + \text{X}) + \frac{1}{2} (D+E) (\text{H} + \text{X})
 \end{aligned}$$

FIG. 23. Diagrammatic calculation of the coefficient of (1, -1). The first step involves redrawing the diagrams. The second and the third steps involve the use of Jacobi's identity and the triangle contraction. Manipulations involving the Z meson must be modified if the group is SU(n) or if the Higgs bosons are not isodoublets.

We have therefore shown that the eigenequation (59) has a solution for arbitrarily large eigenvalues β . However, it is important to realize that some of the eigenvalues may not be relevant for our purpose. Indeed, for the purpose of studying the analytic property of $h_0(\xi, \Delta^2)$ as a function of ξ , we need, according to (48), to express $f_0^{(0)}(\vec{q}_1)$ as a linear superposition of the eigenfunctions of $(2P_1 - P_2)$. Thus we need to include only those eigenfunctions of $(2P_1 - P_2)$ which form a complete set. Let us, therefore, go back to (C17). Setting

$$\tau = \gamma t, \quad \tau' = \gamma t', \tag{C23}$$

and

$$\varphi(\tau) = e^{\tau/2} \phi(\tau), \tag{C24}$$

we transform (C17) into

$$\beta \varphi(\tau) = \int_0^\infty \frac{d\tau'}{2\pi^2} e^{-|\tau-\tau'|/2} \varphi(\tau'). \tag{C25}$$

The kernel in (C25) is the approximation of the kernel of (59) for $\beta \gg 1$. The change of variable (C24) is for the purpose of symmetrizing the kernel. By (C18) and (C24), the eigenfunction of (C25) is

$$\varphi(\tau) = \frac{e^{(1/2-\eta_1)\tau}}{\eta_1} - \frac{e^{(1/2-\eta_2)\tau}}{\eta_2}. \tag{C26}$$

From (C19) and (C20), we find that the eigenfunctions of (C26) with

$$0 < \beta < \frac{2}{\pi^2} \tag{C27}$$

are oscillatory and form a complete and orthogonal set of functions which can be used as a basis for the representation of any square-integrable function defined for $0 \leq \tau \leq \infty$. The eigenfunctions for $\beta > 2/\pi^2$ or $\beta < 0$ blow up exponentially as $\tau \rightarrow \infty$, and are not needed in the representation of a square-integrable function.

Equation (C27) gives the relevant spectrum for the kernel $e^{-|\tau-\tau'|}$ which approximates the kernel of (59) only if $\beta \gg 1$. The interval defined by (C27) does not satisfy $\beta \gg 1$. Thus, in order to select the relevant spectrum of (59), we must use (61) instead of (C19) and (C20), since the latter approximate the roots of (61) only if $\beta \gg 1$. It is then straightforward to show that $(\frac{1}{2} - \eta_1)$ and $(\frac{1}{2} - \eta_2)$ are purely imaginary only if β is in the region defined by (62). When β is outside of this region, the corresponding function $\phi(\vec{q}_1)$, after it is multiplied by $e^{\tau/2}$ as in (C24), blows up as $|\vec{q}_1| \rightarrow \infty$. [Remember, according to (C8) and (C23), that $e^{\tau/2}$ is proportional to $(\vec{q}_1^2)^{1/2}$.] Thus we believe that these eigenvalues are not relevant for the purpose of spectral decomposition.

*Work supported in part by the National Science Foundation under Grant No. PHY76-12396.

¹H. Cheng and T. T. Wu, Phys. Rev. Lett. 24, 1456 (1970). A fairly complete review of these results can be found in H. Cheng, report to the IV International Symposium on Multiparticle Hydrodynamics, Pavia,

Italy, 1973 (unpublished).

²G. 't Hooft and M. Veltman, in *Proceedings of the Colloquium on Renormalization of Yang-Mills Fields and Applications to Particle Physics, Marseille, France, 1972*, edited by C. P. Korthals-Altes (C.N.R.S., Marseille, France, 1972).

³M. Grisaru, H. Schnitzer, and H.-S. Tsao, Phys. Rev. Lett. **30**, 811 (1973).

⁴V. S. Fadin, E. A. Kuraev, and L. N. Lipatov, Phys. Lett. **60B**, 50 (1975).

⁵They were first obtained by B. McCoy and T. T. Wu, Phys. Rev. Lett. **35**, 604 (1975). See also L. Tyburski, Phys. Rev. D **13**, 1107 (1976); B. McCoy and T. T. Wu, *ibid.* **13**, 1076 (1976); H. T. Nieh and Y.-P. Yao, *ibid.* **13**, 1082 (1976); L. L. Frankfurt and V. E. Sherman, Yad. Fiz. **23**, 1099 (1976) [Sov. J. Nucl. Phys. **23**, 581 (1976)].

⁶Strictly speaking, the sum of a convergent integral and a divergent integral is still a divergent integral, and, in general, it is impossible to make a distinction between them. However, it is possible to do so in our case because of the special forms the integrands take. In our case, the denominator of an integrand is in the form of $\Pi_n(\vec{p}_{n\perp}^2 + \lambda^2)$, where $\vec{p}_{n\perp}$ is the transverse momentum of line n and the numerator is a polynomial of $\vec{p}_{n\perp}$, $\vec{\Delta}$, and λ . For a diagram of the second kind, the integral involved is divergent even

if the numerator is set equal to unity, provided that the integrand is in the form such that the numerator and the denominator have no common factors.

⁷C. Y. Lo and H. Cheng, Phys. Rev. D **13**, 1131 (1976).

⁸For W - W scattering, there is confusion in identifying, at each vertex, which of the three W mesons involved is the emitted or the absorbed one. Fortunately, in the high-energy limit, one of the mesons at each vertex always carries a longitudinal momentum much smaller than those of the other two. We shall define this meson as the emitted (or absorbed) one. With this definition, the multi- W -exchange diagrams for W - W scattering are the same as those for fermion-fermion scattering, with the restriction that the top and the bottom horizontal lines carry almost all of the incident momenta.

⁹This has also been independently obtained by T. T. Wu and B. McCoy (private communication with T. T. Wu).

¹⁰A detail account of the generalization to $SU(n)$ is given by P. Yeung, Phys. Rev. D **13**, 2306 (1976). See also L. Tyburski in Ref. 5.